Research Article | Vol. 9, No. 3 | 1 Mar 2018 | BIOMEDICAL OPTICS EXPRESS 984

Biomedical Optics EXPRESS

Application of a near-infrared laser tweezers Raman spectroscopy system for label-free analysis and differentiation of diabetic red blood cells

JINYONG LIN,[1,4] LINGDONG SHAO,[1,4] SUFANG QIU,[1] XINGWU HUANG,[1] MENGMENG LIU,[2] ZUCI ZHENG,[2] DUO LIN,[2] YONGLIANG XU,[2] ZHIHUA LI,[2] YAO LIN,[3] RONG CHEN,[2] AND SHANGYUAN FENG[2,5]

[1]*Department of Radiation Oncology, Fujian Cancer Hospital & Fujian Medical University Cancer Hospital, Fuzhou, Fujian, China*
[2]*Key Laboratory of OptoElectronic Science and Technology for Medicine, Ministry of Education and Fujian Provincial Key Laboratory for Photonics Technology, Fujian Normal University, Fuzhou 350007, China*
[3]*Provincial University Key Laboratory of Cellular Stress Response and Metabolic Regulation, College of Life Sciences, Fujian Normal University, Fuzhou, Fujian Province, 350117, China*
[4]*Jinyong Lin and Lingdong Shao contributed equally to this work*
[5]*syfeng@fjnu.edu.cn*

Abstract: A home-made near-infrared laser tweezers Raman spectroscopy (LTRS) system was applied to detect hemoglobin variation in red blood cells (RBCs) from diabetes without exogenous labeling. Results showed significant spectral differences existed between the diabetic and normal RBCs, including the peaks dominated by protein components (e.g. 1003 cm^{-1}) and heme groups (e.g. 753 cm^{-1}) in RBCs, and accurate classification results for diabetes detection were obtained by linear discriminant analysis with 100% sensitivity (i.e. no false negatives in the study). This work indicated the great promise of LTRS as a label-free RBC analytical tool for improving the accurate detection of type II diabetes.

© 2018 Optical Society of America under the terms of the OSA Open Access Publishing Agreement

OCIS codes: (170.0170) Medical optics and biotechnology; (170.4580) Optical diagnostics for medicine; (170.5660) Raman spectroscopy.

References and links

1. W. H. Organization, "Global report on diabetes," Working Papers (2016).
2. T. Scully, "Diabetes in numbers," Nature **485**(7398), S2–S3 (2012).
3. J. M. Forbes and M. E. Cooper, "Mechanisms of diabetic complications," Physiol. Rev. **93**(1), 137–188 (2013).
4. J. C. Bazo-Alvarez, R. Quispe, T. D. Pillay, A. Bernabé-Ortiz, L. Smeeth, W. Checkley, R. H. Gilman, G. Málaga, and J. J. Miranda, "Glycated haemoglobin (HbA1c) and fasting plasma glucose relationships in sea-level and high-altitude settings," Diabet. Med. **34**(6), 804–812 (2017).
5. D. B. Sacks, M. Arnold, G. L. Bakris, D. E. Bruns, A. R. Horvath, M. S. Kirkman, A. Lernmark, B. E. Metzger, and D. M. Nathan; National Academy of Clinical Biochemistry; Evidence-Based Laboratory Medicine Committee of the American Association for Clinical Chemistry, "Guidelines and recommendations for laboratory analysis in the diagnosis and management of diabetes mellitus," Diabetes Care **34**(6), e61–e99 (2011).
6. K. J. Welsh, M. S. Kirkman, and D. B. Sacks, "Role of Glycated Proteins in the Diagnosis and Management of Diabetes: Research Gaps and Future Directions," Diabetes Care **39**(8), 1299–1306 (2016).
7. I. Barman, N. C. Dingari, J. W. Kang, G. L. Horowitz, R. R. Dasari, and M. S. Feld, "Raman spectroscopy-based sensitive and specific detection of glycated hemoglobin," Anal. Chem. **84**(5), 2474–2482 (2012).
8. D. M. Kim and Y. B. Shim, "Disposable amperometric glycated hemoglobin sensor for the finger prick blood test," Anal. Chem. **85**(13), 6536–6543 (2013).
9. K. Chen, Y. Qin, F. Zheng, M. Sun, and D. Shi, "Diagnosis of colorectal cancer using Raman spectroscopy of laser-trapped single living epithelial cells," Opt. Lett. **31**(13), 2015–2017 (2006).
10. R. Liu, Z. Mao, D. L. Matthews, C. S. Li, J. W. Chan, and N. Satake, "Novel single-cell functional analysis of red blood cells using laser tweezers Raman spectroscopy: application for sickle cell disease," Exp. Hematol. **41**(7), 656–661 (2013).
11. D. Lin, Z. Zheng, Q. Wang, H. Huang, Z. Huang, Y. Yu, S. Qiu, C. Wen, M. Cheng, and S. Feng, "Label-free optical sensor based on red blood cells laser tweezers Raman spectroscopy analysis for ABO blood typing," Opt.

#314235 https://doi.org/10.1364/BOE.9.000984
Journal © 2018 Received 24 Nov 2017; revised 11 Jan 2018; accepted 15 Jan 2018; published 2 Feb 2018

Biomedical Optics EXPRESS

Express **24**(21), 24750–24759 (2016).
12. G. Rusciano, A. C. De Luca, G. Pesce, and A. Sasso, "Raman Tweezers as a Diagnostic Tool of Hemoglobin-Related Blood Disorders," Sensors (Basel) **8**(12), 7818–7832 (2008).
13. J. L. Deng, Q. Wei, M. H. Zhang, Y. Z. Wang, and Y. Q. Li, "Study of the effect of alcohol on single human red blood cells using near-infrared laser tweezers Raman spectroscopy," J. Raman Spectrosc. **36**(3), 257–261 (2005).
14. A. J. Berger, T. W. Koo, I. Itzkan, G. Horowitz, and M. S. Feld, "Multicomponent blood analysis by near-infrared Raman spectroscopy," Appl. Opt. **38**(13), 2916–2926 (1999).
15. B. R. Wood, P. Caspers, G. J. Puppels, S. Pandiancherri, and D. McNaughton, "Resonance Raman spectroscopy of red blood cells using near-infrared laser excitation," Anal. Bioanal. Chem. **387**(5), 1691–1703 (2007).
16. J. Zhao, H. Lui, D. I. McLean, and H. Zeng, "Automated autofluorescence background subtraction algorithm for biomedical Raman spectroscopy," Appl. Spectrosc. **61**(11), 1225–1232 (2007).
17. Z. Huang, A. McWilliams, H. Lui, D. I. McLean, S. Lam, and H. Zeng, "Near-infrared Raman spectroscopy for optical diagnosis of lung cancer," Int. J. Cancer **107**(6), 1047–1052 (2003).
18. J. Lin, Z. Huang, S. Feng, J. Lin, N. Liu, J. Wang, L. Li, Y. Zeng, B. Li, H. Zeng, and R. Chen, "Label-free optical detection of type II diabetes based on surface-enhanced Raman spectroscopy and multivariate analysis," J. Raman Spectrosc. **45**(10), 884–889 (2015).
19. B. R. Wood and D. Mcnaughton, "Raman excitation wavelength investigation of single red blood cells in vivo," J. Raman Spectrosc. **33**(7), 517–523 (2002).
20. A. Bankapur, E. Zachariah, S. Chidangil, M. Valiathan, and D. Mathur, "Raman Tweezers Spectroscopy of Live, Single Red and White Blood Cells," PLoS One **5**(4), e10427 (2010).
21. J. Lin, J. Lin, Z. Huang, P. Lu, J. Wang, X. Wang, and R. Chen, "Raman spectroscopy of human hemoglobin for diabetes detection," Journal of Innovation in Optical Health Science **7**, 697 (2014).
22. J. Lin, G. Cao, J. Lin, N. Liu, F. Liao, Q. Ruan, S. Wu, Z. Huang, L. Li, and R. Chen, "Serum albumin analysis for type II diabetes detection using surface-enhanced Raman spectroscopy," Proc. SPIE **9230**, 92301Z (2014).
23. J. Wang, S. Feng, J. Lin, Y. Zeng, L. Li, Z. Huang, B. Li, H. Zeng, and R. Chen, "Serum albumin and globulin analysis for hepatocellular carcinoma detection avoiding false-negative results from alpha-fetoprotein test negative subjects," Appl. Phys. Lett. **103**, 837–866 (2013).
24. S. K. Teh, W. Zheng, K. Y. Ho, M. Teh, K. G. Yeoh, and Z. Huang, "Near-infrared Raman spectroscopy for gastric precancer diagnosis," J. Raman Spectrosc. **40**(8), 908–914 (2010).
25. S. Li, Y. Zhang, J. Xu, L. Li, Q. Zeng, L. Lin, Z. Guo, Z. Liu, H. Xiong, and S. Liu, "Noninvasive prostate cancer screening based on serum surface-enhanced Raman spectroscopy and support vector machine," Appl. Phys. Lett. **105**, 57–136 (2014).
26. J. W. Baynes, "Role of oxidative stress in development of complications in diabetes," Diabetes **40**(4), 405–412 (1991).
27. L. Razzouk, V. Mathew, R. J. Lennon, A. Aneja, J. I. Mozes, H. J. Wiste, P. Muntner, J. H. Chesebro, and M. E. Farkouh, "Power dependent oxygenation state transition of red blood cells in a single beam optical trap," Appl. Phys. Lett. **99**, 671 (2011).
28. J. Lin, Y. Zeng, J. Lin, J. Wang, L. Li, Z. Huang, B. Li, H. Zeng, and R. Chen, "Erythrocyte membrane analysis for type II diabetes detection using Raman spectroscopy in high-wavenumber region," Appl. Phys. Lett. **104**(10), 104102 (2014).
29. D. Lin, G. Chen, S. Feng, J. Pan, J. Lin, Z. Huang, and R. Chen, "Development of a rapid macro-Raman spectroscopy system for nasopharyngeal cancer detection based on surface-enhanced Raman spectroscopy," Appl. Phys. Lett. **106**(1), 013701 (2015).
30. G. Del Mistro, S. Cervo, E. Mansutti, R. Spizzo, A. Colombatti, P. Belmonte, R. Zucconelli, A. Steffan, V. Sergo, and A. Bonifacio, "Surface-enhanced Raman spectroscopy of urine for prostate cancer detection: a preliminary study," Anal. Bioanal. Chem. **407**(12), 3271–3275 (2015).
31. K. Lin, D. L. P. Cheng, and Z. Huang, "Optical diagnosis of laryngeal cancer using high wavenumber Raman spectroscopy," Biosens. Bioelectron. **35**(1), 213–217 (2012).
32. G. R. Lloyd, L. M. Almond, N. Stone, N. Shepherd, S. Sanders, J. Hutchings, H. Barr, and C. Kendall, "Utilising non-consensus pathology measurements to improve the diagnosis of oesophageal cancer using a Raman spectroscopic probe," Analyst (Lond.) **139**(2), 381–388 (2014).
33. R. Bro and A. K. Smilde, "Principal component analysis," Anal. Methods **6**(9), 2812–2831 (2014).
34. K. Lin, D. L. Cheng, and Z. Huang, "Optical diagnosis of laryngeal cancer using high wavenumber Raman spectroscopy," Biosens. Bioelectron. **35**(1), 213–217 (2012).
35. S. Feng, J. Lin, Z. Huang, G. Chen, W. Chen, Y. Wang, R. Chen, and H. Zeng, "Esophageal cancer detection based on tissue surface-enhanced Raman spectroscopy and multivariate analysis," Appl. Phys. Lett. **102**(4), 043702 (2013).
36. N. A. Obuchowski, "Receiver Operating Characteristic Curves and Their Use in Radiology," Radiology **229**(1), 3–8 (2003).

1. Introduction

Diabetes has become an important public health problem recently with an estimated 422 million adults living with it in the world [1]. Sadly, diabetes caused almost 1.5 million deaths globally within one year [1, 2]. Type II diabetes (*i.e.* the non-insulin-dependent diabetes)

Biomedical Optics EXPRESS

accounts for the majority (nearly 85%) of people with diabetes worldwide [3]. In addition, the symptoms of type II diabetes are often less marked or absent [1]. So the disease may go undiagnosed for years, until complications (e.g. heart attack, kidney failure, nerve damage and so on) have already arisen, which increases the overall risk of dying prematurely [1]. Early diagnosis plays an important role in decreasing the complications and increasing patient survival. Nowadays, the tests of glycated hemoglobin (HbA1c) and blood glucose are regular methods for diabetes detection [4]. Especially, HbA1c, which is formed by the nonenzymatic glycation of hemoglobin exposed to high blood glucose, is significantly correlated with the average glucose level in the preceding 3 months period (life span of the RBCs) [5, 6]. Compared with glucose test, HbA1c test has several advantages, such as low intraindividual variation and no demand for fasting [4], which make it is increasingly accepted as clinically stable and reliable index for type II diabetes screening.

Currently, HbA1c test is conducted by assay techniques, including immunoassay, boronated affinity chromatography (BAC), high performance liquid chromatography (HPLC) and so on [7, 8]. However, these methods have certain inadequacies, such as the long time for the analysis, the complicated operation for cell lysis and antibody-based labeling, and the need for invasive exogenous reagent and big sample volume [8]. Considering hemoglobin is the major contents of RBC, development of a convenient, label-free and micro-sample screening technique via direct RBC analysis would be of great clinical value for type II diabetes identification.

Laser tweezers Raman spectroscopy (LTRS), which combines laser tweezers technique and Raman detection, enables the capture, manipulation, and biomolecular fingerprinting of individual live cell without exogenous labeling of the sample [9]. Briefly, an optical trap (i.e. laser tweezers) formed by a focused laser beam is used to capture a cell without disrupting its biological activity. Then the Raman spectrum is obtained simultaneously by the same laser, providing structure and composition information at the molecular level [10]. To date, many studies have demonstrated the applications of LTRS for RBC detection in biomedical field [10–12]. However, LTRS for the detection of RBCs variation in diabetes progression has not been reported.

The main focus of this article is to evaluate the potential of applying LTRS technique for label-free analysis of RBC samples belonging to diabetic and normal subjects for type II diabetes determination. The principal component analysis and linear discriminant analysis (PCA-LDA) multivariate methods are utilized to analyze and discriminate the RBCs spectra acquired from the two groups. This primary study may develop a reagent-free and reliable method for type II diabetes screening, which can be performed on micro-sample volume with the need for little or no sample preparation.

2. Materials and methods

2.1 Samples collection and preparation

Table 1. Clinical Information on Type II Diabetes and Healthy Volunteers

	Type II Diabetes (n = 45)	Healthy Volunteers (n = 45)
Age		
Mean	53 ± 9	46 ± 16
Gender		
Male	19	22
Femal	26	23
Clinical examination		
HbA1c value	6.6~12.8%	< 6.5%
Fasting plasma glucose	7.8~13.8 mmol/L	< 7.0 mmol/ L

In this study, totally 90 blood samples were drawn from two subject groups: one with clinical diagnosis of type II diabetes (HbA1c value ≧ 6.5% and on medication, n = 45) and the other consisted of healthy volunteers (n = 45). The detailed information on subjects can be found in

Biomedical Optics EXPRESS

Table 1. In the study, 90 blood samples (45 diabetic and 45 healthy) were divided into a calibration set (35 diabetic and 35 healthy) and a validation set (10 diabetic and 10 healthy) for statistical analysis. All blood samples were from the First Hospital of Fuzhou, and the research was approved by the ethical committee in the hospital. For preparation of RBCs samples, the whole blood samples were centrifuged to remove white cells and other impurities. To purify the RBCs, the cells were washed with 0.9% physiological saline and were diluted with it. At last, 2 ml aliquot of the diluted RBCs suspension liquid was pipetted into a quartz-bottom culture dish which was placed on the LTRS microscope platform for single-RBC detection. For each sample, at least 10 RBCs were analyzed and averaged to obtain each data point. To emphasize the low intraindividual variability of RBCs, we randomly divided 20 RBCs' spectra from a blood sample into two groups on average. Obviously, there are not significant different ($p<0.05$) peaks between the two group, indicating intraindividual variability of RBCs from the same blood sample is low.

2.2 Experimental set-up

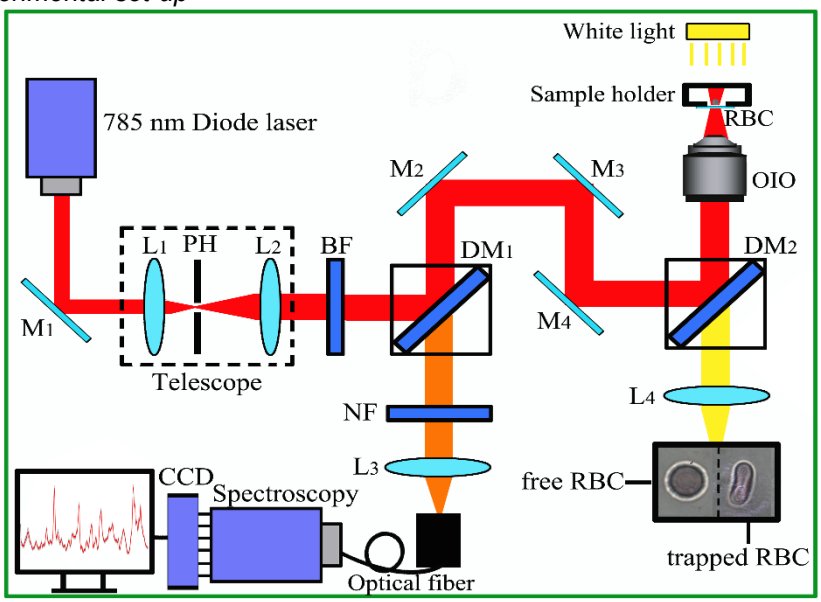

Fig. 1. Principle of our home-made near-infrared LTRS system, in which a 785 nm laser beam is focusd into an optically trap for capturing cell and is simultaneously used to obtain Raman spectrum of the trapped cell. Abbreviation: M-mirror; L-lens; PH-pinhole; DM-dichroic mirror; NF-notch filter; OIO-oil immersion objective; RBC-red blood cell; Hb-hemoglobin.

A home-made near-infrared laser tweezers Raman spectroscopy (LTRS) system was employed for this study. Figure 1 showed the schematic illustration of the system. In detail, the diode laser beam at 785 nm was firstly passed through a telescopic system (comprised of lenses L_1, L_2, and 10 um pinhole) to obtain a circular beam with approximately 6 mm diameter. Then after being spectrally filtered by a band pass filter, the laser beam was delivered into an oil immersion objective (100 × , 1.30 numerical aperture) equipped in an inverted Olympus microscope system (IX71; USA) to be focused as a single-beam optical trap above the sample holder. In particular, the sample holder is a self-modified culture dish with a drilled hole sealed by a 80 μm thick quartz slide at the center. By moving the manual stage, one RBC in the aqueous solution could be isolated and immobilized within the beam focus at 20 μm height above the quartz slide. For real-time monitoring, the RBC was illuminated by a white light which imaged the cell (inserted pictures in Fig. 1) on a video camera system through a dichroic mirror (DM_2 in Fig. 1). Here, the DM_2 can reflect near-

infrared radiation and be transparent to visible radiation. At the same time, the same laser also served as the excitation source for obtaining Raman spectrum of the trapped RBC. The benefit of choosing 785 nm as the Raman excitation light is that near-infrared region can weaken photo-damage to the trapped cell and can efficiently suppress fluorescence background, and is widely employed for blood component analysis in biomedical field [13–15]. The backscattering photons from the trapped RBC passed along the same optical pathway and were filtered through the dichroic mirror (DM1 in Fig. 1) which would reflect 785 nm radiation and be transparent to scattering radiation. Ultimately, the Raman scattering photons purified by holographic notch filter were collected and transmitted to a spectrograph (Holospec-f/2.2-NIR, Kaiser) coupled to a charge-coupled device detector (1024 × 256 pixels, Princeton Instruments) using a 50 μm diameter single-fiber. Here, the single-fiber is equivalent to a 50 μm pinhole, enabling the elimination of stray light to a great extent. In the study, LTRS system was calibrated by a silicon wafer at 520 cm^{-1} band, and the Raman spectra were acquired from 420 to 1700 cm^{-1} region with 5 mW laser power and 40 s integration time. Raw spectral data were preprocessed with a fifth-order multi-polynomial fitting algorithm [16] to remove the fluorescence background. After fitting, each Raman spectrum was normalized or scaled by dividing by the integrated area under the curve in the spectral range of 420-1700 cm^{-1} by Origin Pro 8.0 software package. By this way, the absolute intensity of spectral bands was replaced with relative intensity (i.e. percentage signals intensity); thus, the absolute intensity variations from possible laser fluctuations can be reduced, promoting a better comparison of spectral patterns and percentage signal of various Raman bands between diabetic and normal RBCs samples [17].

3. Results and discussion

3.1 Raman spectra

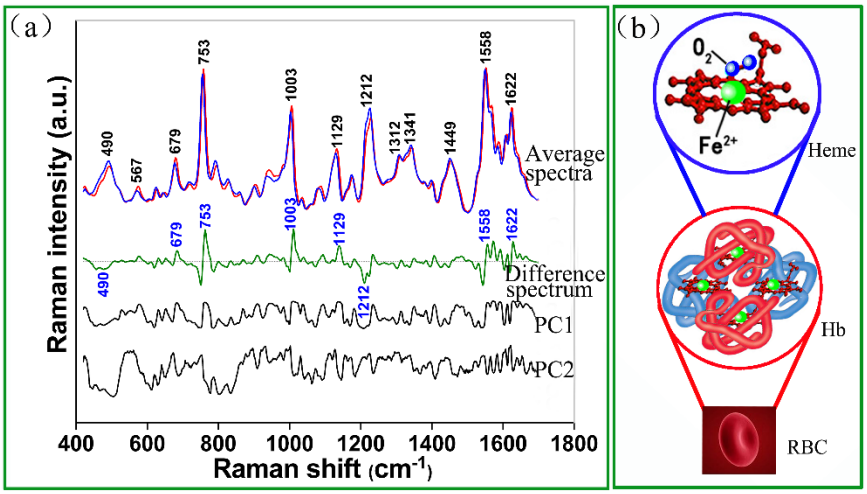

Fig. 2. (a) Red and blue curves: the average Raman spectra of type II diabetic (red curve) and normal (blue curve) RBCs; Green curve: the difference spectrum (diabetic minus normal). Black curves: the 1st and 2nd principal components (PC1 and PC2), respectively, which are most diagnostically significant for diabetes detection (scaled by a factor 0.1). (b) Structural schematic of the hemoglobin in the red blood cell. RBC-red blood cell; Hb-hemoglobin.

Biomedical Optics EXPRESS

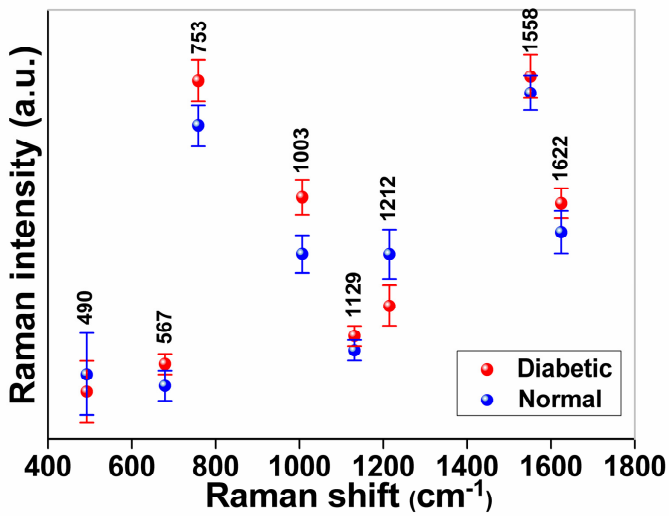

Fig. 3. The mean intensities and standard deviations of the RBC Raman bands with major variations ($p<0.05$) from normal to diabetic.

Table 2. The spectral assignments for RBC.

Raman shift (cm^{-1})	Assignment [a,b]
490	p: S-S str
567	ν(Fe-O)
679	δ(pyr deform) $_{sym}$
753	ν(pyr breathing)
1003	Phenylalanine
1129	ν($C_β$-methyl)
1212	δ(C_mH)
1312	$ν_{21}$, δ(C_mH)
1341	ν(pyr half-ring)$_{sym}$
1449	p: δ(CH_2/CH_3)
1558	ν($C_βC_β$)
1622	ν(C = C)$_{vinyl}$, ν(C_a = C_b)

[a] Notes: ν, stretch; δ, bend/scissor; sym, symmetric; p: protein; pyr, porphyrin;

[b] Assignments taken from References [11, 15, 18–21].

Figure 2(a) showed the normalized average Raman spectra of the 35 type II diabetic (red curve) and 35 normal (blue curve) RBCs in training set. The average spectra exhibited prominent characteristic of RBCs at 490, 567, 679, 753, 1003, 1129, 1212, 1312, 1341, 1449, 1558, and 1622 cm^{-1}. The spectral assignments were listed in Table 2, according to the previous research [11, 15, 18–21]. The spectra contained most information related to the porphyrin macrocycles and various protein components of hemoglobin which is the major contents of RBCs (one RBC contains ~2.5×10^8 hemoglobin molecules). As shown in Fig. 2(b), hemoglobin is a tetramer made of four heme groups attached with their respective globin chain (two α-like chains and two β-like chains) [18]. For each heme, there is one Fe ion which serves as O_2-binding site in the center of the porphyrin rings [13]. To highlight the spectral differences between the two groups, the difference spectrum (green curve, diabetic minus normal) was shown in Fig. 2(a). The major variations ($p<0.05$) from normal to diabetic

were the increased Raman intensities at 679 (porphyrin symmetric deformation mode), 753 (porphyrin breathing vibration mode), 1003 (Phenylalanine), 1129 (C_β-methyl stretching mode), 1558 ($C_\beta C_\beta$ stretching mode) and 1622 cm^{-1} (C = C vinyl and C_a = C_b stretching mode), and the decreased ones at 490 (S-S stretching mode) and 1212 cm^{-1}(C_mH bending mode). Figure 3 is a plot of the intensity values of these different peaks and their mean values with associated standard deviations. These variations showed the constituent and conformational changes of hemoglobin in RBC after exposed to high blood glucose for a long period of time. For instance, the higher spectral intensity of phenylalanine (at 1003 cm^{-1}) for the diabetes suggested there was an increase of phenylalanine content relative to the total Raman-active components in diabetic RBCs, which was in accordance with our previous study on serum albumin of diabetic patients [22]. Besides, many studies also have reported that the phenylalanine band would change when people in an abnormal medical condition [23–25]. The band at 753 cm^{-1} (porphyrin breathing mode), which is the direct indicator of heme status in RBCs [13], exhibits higher signal in diabetes, indicating the enhancement of porphyrin breathing mode in diabetic RBCs. The reason for this enhancement may be ascribed to the change of oxidation environment in RBCs considering the vibration is sensitive to oxygen [15]. Similarly, the decreased band at 1212 cm^{-1} and the increased bands at 1558 and 1622 cm^{-1}, which are the marker for oxygenation, also indicates the difference of oxygenation state between diabetic and normal RBCs. Two possible mechanisms for the dissimilarity of oxygenation state were proposed: one may be the peroxidation and free radical reaction in high concentration of blood glucose [26]; the other may be the different oxygenation response of diabetic and normal RBCs to an applied mechanical force imposed by the optical trap [10, 27]. However, considering oxygenation state of hemoglobin may be interfered by some external factor (e.g. the time for blood extraction and the dissolved oxygen in the diluted solution), more rigidly controlled experiments for taking samples and testing need to be carried out to further clarify the oxygenation-induced effects on diabetic RBC Raman spectra in our future study. In addition, it needs to be pointed out that these variations in the spectral intensities were basically consistent with our previous study on using Raman spectroscopy to directly analyze human hemoglobin isolated from diabetic and normal RBCs [21]. Furthermore, Barman group also observed these subtle but discernible spectral shape differences in their research on Raman spectroscopy-based sensitive and specific detection of glycated hemoglobin (purely commercial sample) [7]. Thus, as explained by Barman group [7], these spectral variation may be also ascribed to structural changes in hemoglobin related to the binding of a glucose moiety (i.e. nonenzymatic glycosylation of hemoglobin [6]). So these reproducible variations in Raman spectra between normal and diabetic RBCs suggested the potential of the LTRS for rapid and efficient detection of type II diabetes.

3.2 PCA-LDA statistical analysis

In order to efficiently utilize finite spectral differences between diabetic and normal groups for diabetes detection, PCA-LDA statistical algorithm was implemented on the measured Raman spectra by SPSS 15.0 software package (SPSS Inc. Chicago). As a powerful spectral analytical tool, this algorithm has been universally employed to promote the efficiency of Raman spectroscopy for disease diagnosis [28–32]. In present work, principal component analysis (PCA), a dimensional-reduction technique by transforming complex data variables to a minimal set of orthogonal variables called principal components (PCs) that explained the maximum data variance, was firstly used to the raw spectral data (420-1700 cm^{-1}) to generate a few PCs, followed by independent-sample T test [33]. Results showed that two PCs (PC1 and PC2) were diagnostically significant for distinguishing diabetic from normal RBCs using the definition of $p < 0.05$ [34]. Black Curves in Fig. 2(a) are the loading plots of PC1 and PC2. It was clear that PC1 and PC2 shared most spectral bands in the difference spectrum (green curve in Fig. 2(a)), including 490, 679, 753, 1003, 1129, 1212, 1558, and 1622 cm^{-1}, which were diagnostically relevant spectral bands. Then, these two most significant PC scores (PC1

Biomedical Optics EXPRESS

and PC2) were loaded into the linear discriminant analysis (LDA) algorithm which could maximize the ratio of between-class variance to within-class variance in a data set to figure out the discriminant equation that best distinguish the diabetic RBCs from the normal ones [35]. The discriminant equation was as follows:

$$1.135PC1 - 0.661PC2 - 0.045 = 0$$

To self-test the performance of the diagnostic model (i.e., the calibration stage), the discriminant equation was retrospectively put into use in the calibration set (35 diabetic and 35 normal). Figure 4(a) showed the corresponding PCA scatter plot of the calibration data set (PC1 and PC2 are the x-axes and y-axes, respectively). Obviously, the diabetic (red circle) and normal data sets (blue circle) were largely clustered into two separate regions, which suggested that the RBCs Raman spectra were able to discriminate diabetic from normal group. Discrimination results (in Fig. 4(b)) showed that the sensitivity and specificity of the calibration model for diabetes detection were 100% (35/35) and 97.1% (34/35), respectively. The derived receiver operating characteristic (ROC) curve (in Fig. 4(c)), which is the plot of tests' sensitivities versus their false-positive rates for all possible threshold levels [36], is another measure of the model's ability for diabetes detection. The area under the ROC is positively related with the discriminant accuracy [36]. Here, the area under the ROC was 0.999, fairly close to 1, implying a relatively ideal calibration model.

In a prospective application study using the diagnostic model (i.e., the validation stage), double-blind test was performed on the additional 10 diabetic and 10 normal subjects in validation data set. After loading spectral data into the above diagnostic model, agreements with clinical diagnosis were reached for 10 out of 10 diabetic and 9 out of 10 normal samples, corresponding to 100% sensitivity and 90% specificity (shown in Fig. 4(d), 4(e)). Besides, the area under the ROC curve was 1.00 (in Fig. 4(f)). These discrimination results were summarized in Table 3. This work indicated the promising potential of LTRS as a label-free analytical tool for the functional, structural analysis of individual RBC for promoting the accurate detection of type II diabetes based on micro-sample volume.

Table 3. Discrimination results of the calibration and validation data set for diabetes detection using RBCs LTRS combined with PCA-LDA

Data sets	Selected PCs	Sensitivity (%)	Specificity (%)	ROC areas
Calibration group	PC1 and PC2	100 (35/35)	97.1 (34/35)	0.999
Validation group	PC1 and PC2	100 (10/10)	90 (9/10)	1.00

Biomedical Optics EXPRESS

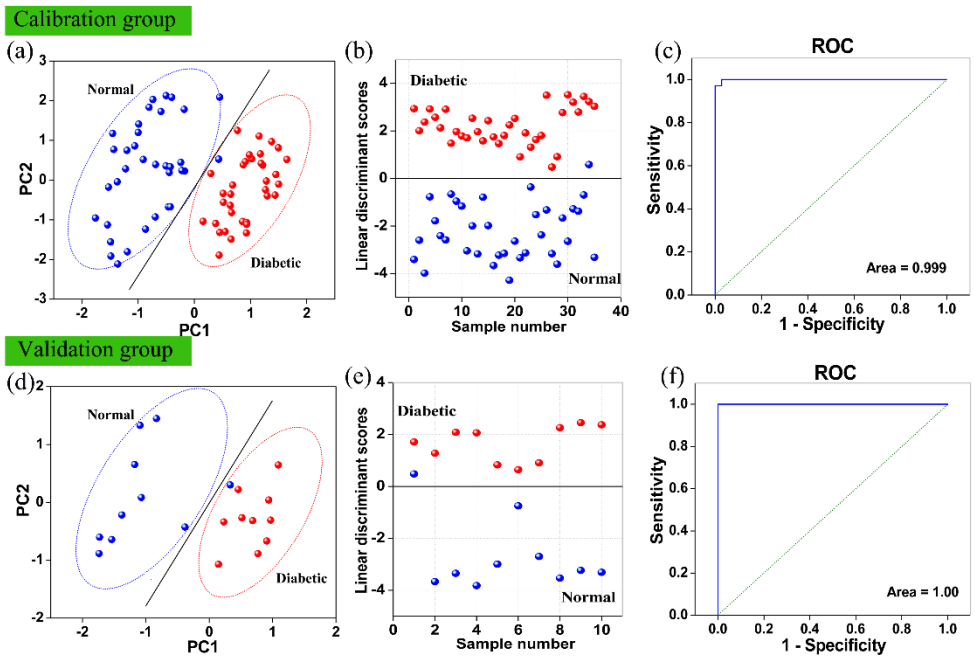

Fig. 4. Statistical analysis for the calibration data set (35 diabetic and 35 healthy samples): (a) PCA plots of the RBCs Raman data belonging to the type II diabetic group (red circle) and the healthy group (blue circle). (b) Scatter plots of the LDA scores, drawing the sensitivity of 100% (35/35) and specificity of 97.1% (34/35) for diabetes detection. (c) The derived receiver operating characteristic (ROC) curve, yielding the integrated area of 0.999. Statistical results for the validation data set (10 diabetic and 10 healthy samples): (d) PCA plots of the RBCs Raman data belonging to the type II diabetic group (red circle) and the healthy group (blue circle). (e) Scatter plots of the LDA scores, drawing the sensitivity of 100% (10/10) and specificity of 90% (9/10) for diabetes detection. (f) The integrated area under the ROC curves is 1.00.

4. Conclusion

In conclusion, a self-built near-infrared laser tweezers Raman spectroscopy (LTRS) system was applied to analyze single living RBC on the micro-sample from type II diabetic and healthy subjects without disrupting its biological activity. Upon analyzing RBC Raman spectra of the two groups, the changes in proteinous components and heme's oxygenation state of hemoglobin in diabetic RBCs were found. By statistically treating with PCA-LDA, RBC Raman spectra gave out an accurate discrimination result for diabetes detection with a sensitivity of 100%, indicating the great potential of LTRS as a label-free and sensitive analytical tool for the functional, structural analysis of individual RBC for promoting the accurate detection of type II diabetes based on micro-sample volume. Meanwhile, considering the long-term condition for diabetes which needs frequent detection, our proposed method based on micro-sample volume with little need or no sample preparation, may be more convenient, comfortable, and humanity for diabetes detection. Next step, we will focus on measuring more Raman spectra from more diabetic and normal RBC specimens to further verify the reliability of this new detection method for clinical application.

Funding

National Natural Science Foundation of China (Nos. 61575043, 61405036 and 61308113); Scientific Research Innovation Team Construction Program of Fujian Normal University (No. IRTL1702); Major Projects Of International Cooperation (No. 61210016); and Strait United Fund (U1605253); Program for Changjiang Scholars and Innovative Research Team in

Biomedical Optics EXPRESS

University (No. IRT1115); Natural Science Foundation of Fujian Province of China (grant no. 2016J01292); National Clinical Key Specialty Construction Program ([2013]-544), Key Clinical Specialty Discipline Construction Program of Fujian ([2012]-149).

Acknowledgments

We thank Fuzhou First Hospital for providing diabetes blood samples.

Disclosures

The authors declare that there are no conflicts of interest related to this article.